Received: October 23, 2024. Revised: December 15, 2024.

International Journal of
Intelligent Engineering & Systems

http://www.inass.org/

Enhanced Solar Defect Detection via Deep Learning: A CNN-Wavelet Transform-LSTM Approach

Rawad Almashhadani[1]* Goh Chin Hock[2] Farah Hani Bt Nordin[1]
Hazem Noori Abdulrazzak[3] Zaid Ali Abbas[4]

[1]*Institute of Sustainable Energy, Universiti Tenaga Nasional, Kajang, Selangor, Malaysia*
[2]*Institute of Power Engineering, Universiti Tenaga Nasional, Kajang, Selangor, Malaysia*
[3]*Computer Communication Engineering Department, Al-Rafidain University College, Baghdad, Iraq*
[4]*Dep.of Electrical and Electronics Engineering, Faculty of Engineering, Universiti Putra, Selangor, Malaysia*
* Corresponding author's Email: rawadahmed2000@gmail.com

Abstract: Nowadays the efficiency of solar energy generation is compromised by the different kinds of solar defects occurred due to regular operations or environmental conditions. Such defects can be visualized by electroluminescence (EL) images. Recently various techniques introduced which are based on image processing and machine learning functions using the EL images. The conventional machine learning methods are semi-automatic which needs the hand-crafted features extraction. In this paper, the automatic solar defect detection and classification proposed using deep learning. The proposed methodology consists of three phases which are Pre-processing, Feature Extraction and Reduction, and Classification. Convolution Neural Network (CNN) based features extraction and reduction, and Long-Short-Term-Memory (LSTM) for the classification of solar defects are used. In the pre-processing phase, the distortion correction algorithm introduced to remove the distortions using the special kind of Gaussian filtering and improve the contrast. The distortion correction helps to estimate the more robust and reliable features during the CNN which deliver the improved accuracy of detection. This paper enhances the existing CNN-based feature extraction process by incorporating Wavelet Transform (WT) for improved feature representation and applying Principal Component Analysis (PCA) for feature reduction. This optimization reduces the high-dimensional feature vectors into compact, unique, and smaller-sized representations, enabling more efficient and accurate defect detection. The proposed model in this paper, called D-CNN-WT-P-LSTM, is simulated and evaluated with recent deep learning and conventional machine learning methods. The proposed model, D-CNN-WT-P-LSTM, outperforms existing methods, achieving accuracy improvements of 14% and 20% for 2-class and 13% and 11% for 4-class compared to DCNN and CNN models, respectively.

Keywords: Convolution neural network, Deep learning, Electroluminescence, Features reduction, Defect detection, Solar cell, Wavelet transform.

1. Introduction

The renewable energies playing the important role to address the growing demand of power supply along with the environment protection in recent past. The solar farms produce the solar energy and hence it is rapidly growing technology that offers the eco-friendly power supply. However, solar energy generation efficiency is compromised by the different kinds of solar defects occurred due to regular operations or environmental conditions. Such detected effectively visualized by the EL imagining techniques [1]. EL is the electrically determined emanation of light from non-crystalline natural materials, which was first watched and widely concentrated during the 1960s. In 1987, a group in Kodak presented a twofold layer natural light-emanating gadget (OLED), which joined current slim film statement procedures with reasonable materials and structure to give modestly low predisposition voltages and appealing luminance productivity. In 1990 new directing polymer-based LED appeared [2].

Received: October 23, 2024. Revised: December 15, 2024.

From that point forward, there have been expanding interests and research exercises right now and colossal advancement have been made in the upgrades of shading range, luminance productivity and gadget unwavering quality [3]. The developing interest is largely roused by the guarantee of the utilization of this innovation in level board shows. As a result, different OLED shows have been illustrated.

As talked about before, utilizing solar imaging, it is conceivable to envision deserts like splits and inert cell zones to assess the cell productivity and the general module and sunlight-based park area. As machine vision grows quickly, a picture-based imperfection discovery technique has been utilized for sun powered cells regulation in assembling company [4]. Sunlight based cell surface properties assessment cannot just improve the creation nature of the sun-oriented cell module, yet in addition increment the lifetime of the sun powered cell module. For the most part, the raw materials used to make solar cells are divided into monocrystalline silicon and polysilicon. The silicon is monocrystalline sun powered cell has a balanced foundation surface [5]. To dependably acquire the surface deformity attributes, some component extraction strategies are powerful when picture force consistency is fulfilled. The current surface deformity discovery strategies dependent on computer vision can be characterized into 4 classifications in terms of surface highlights: 1) non-finished surface; 2) rehashed design surface; 3) homogeneously finished surface; 4) non-homogeneously-finished surface. However, using these approaches leads to semi-automatic process of defect detection with limited scope. The machine learning techniques using deep learning gained significant attentions due to automatic learning and detection functionality. The recently few studies proposed for the deep learning based (using CNN model) solar defect detection according to different configuration of CNN; however the yet complete research problems to solve.

The key challenge of solar cell manufacturing to generate the eco-friendly solar energy is multiple and indeterminate detection of detects on solar cell exterior with presence of uneven texture and a complicated background. The existing methods focused on directly automated features extraction and detection of using CNN based deep learning models but does not address the challenge of defects detection under the complex and heterogeneous texture. Additionally, the current CNN models are based on automated features extraction process which may not be the reliable by considering the solar surface images variations and hence it is required to optimize the automatic process of features extraction using CNN. Additionally, the current techniques mainly focused on defects detection, however for further analysis purpose it is important to classify the detected defect into the type detect as well. In this paper we presented a novel framework of automatic solar cell detect detection using the optimized deep learning model called D-CNN-WT-P-LSTM, which consist of contributions such as:

- Distortion correction of input solar cell images and improving the quality of poor cell regions to enhance the detection performance using various filtering methods.
- CNN features extraction process improved by addition of wavelet transform to estimate the more reliable and robust features and further select the unique features using the PCA. This block is called as CNN-WT-P which is designed for automatic features extraction.
- The LSTM introduced to perform the sequential learning and classification.

The rest of this paper is organized as follows: Section 2 provides the review of various related works in literature; Section 3 provides the design of proposed methodology; Section 4 provides the simulation results and evaluation; and finally, Section 5 provides the conclusion and Future work.

2. Related works

Since from last decade, several image processing-based techniques introduced for solar-cell detect detection using semi-automated and automated approaches. In [6-15] various techniques based on semi-automatic defect detection proposed. The authors in [6] propose a thermal imaging-based fault detection method for PV systems using the SLIC super-pixel strategy. It enhances detection accuracy, provides timely alerts, and is adaptable but faces challenges with environmental sensitivity, scalability, and limited fault types.

In [7], the authors propose an image-processing method to detect broken corners and black edges in solar cells, improving quality and reducing defects. While efficient and practical for industrial use, it faces limitations in scalability, reliance on high-quality images, and sensitivity to environmental factors like lighting.

In [8], the authors propose a surface defect detection algorithm using MobileNet-SSD, a lightweight deep learning model for real-time applications. It offers efficient and accurate defect detection, making it suitable for mobile and resource-constrained environments. However, it relies on pre-trained models, struggles with complex defects, and is sensitive to environmental factors like lighting.

In [9], the authors propose an automated defect detection system for silicon solar cells using EL imaging and machine learning. While it improves production efficiency and reduces manual inspection, the method is sensitive to environmental factors, relies on high-quality data, and faces scalability challenges in high-speed production.

In [10], the authors present a method for robust segmentation of dislocation defects in polysilicon wafer images, improving defect detection in complex backgrounds. While effective for quality control, the method faces challenges with image quality, computational complexity, scalability, and generalization to other defects or materials.

In [11], the authors introduce a pseudo-colorization technique for EL images of multi-crystalline silicon solar cells to enhance defect detection. While it improves defect visibility, the method is limited by image quality, may amplify noise, and is computationally challenging for large-scale production.

In [12], the authors introduce a novel feature descriptor for classifying defects in multi-crystalline solar cells, improving defect detection and quality control. However, it faces challenges with high-quality image requirements, feature extraction complexity, scalability for large-scale production, and adaptation to new defect types.

In [13], the authors explore the use of machine learning (ML) to optimize solar cell design and fabrication, improving efficiency and reducing costs. While promising, the method faces challenges with large datasets, training complexity, model transparency, adaptation to new materials, and integration into existing manufacturing processes.

In [14], the authors propose a weakly supervised segmentation method for detecting cracks in solar cells using a normalized Lp norm. This approach improves detection accuracy without requiring pixel-level annotations, but it depends on high-quality images, may struggle with background variations, and has challenges in generalizing to different defect types or environments.

In [15], the authors propose a machine learning method to classify defects in EL images of photovoltaic panels, improving defect detection and quality control. However, the method relies on high-quality images, requires extensive annotated data, and may struggle with generalization, interpretability, and background variations.

As the progressive advantages of deep learning technology, recently deep learning based automated solar cell defect detection strategies designed in [16–25]. This method discusses various approaches to identifying and detecting surface deformities and defects in solar cells using deep learning techniques. The methods span several research studies and include the following highlights:

1. Deep Belief Networks (DBNs): Used to initialize network weights by training on sample features, enabling a foundation for detecting surface deformities.
2. Deep Learning and Neural Networks: Various studies proposed using CNNs for fully automated defect classification from EL images, including CNNs with specific architectures, such as GoogleNet and lightweight CNNs, tailored for high accuracy and efficiency. Neural algorithms and multi-spectral CNNs were employed to adjust system parameters for improved defect mapping and classification.

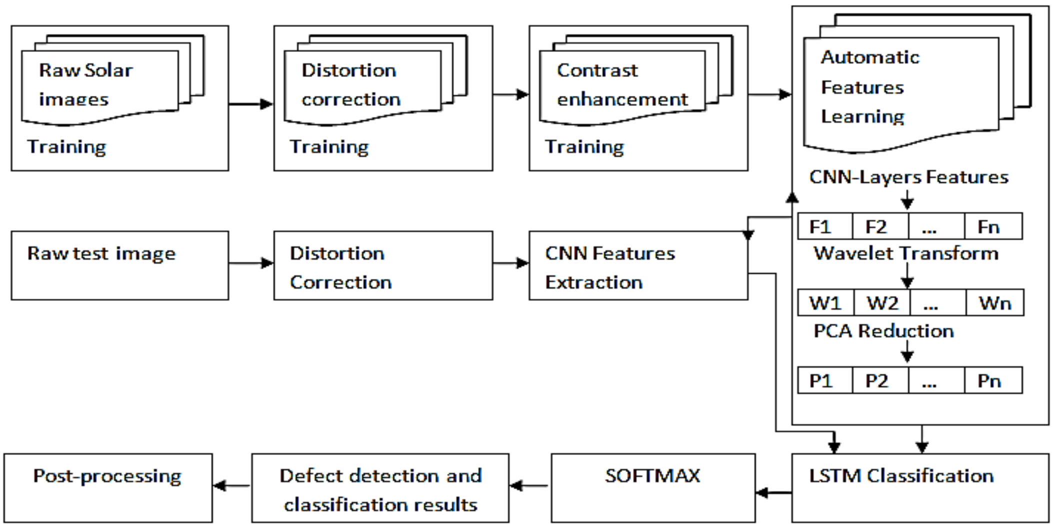

Figure. 1 Proposed automatic deep learning-based solar cell defect system

3. Image Processing and Classification Pipelines: Techniques involve extracting individual cells from module images, analyzing light spectrum features, and applying pre-trained networks for defect identification.
4. Performance Improvements and Hardware Considerations: Approaches range from hardware-efficient Support Vector Machines (SVMs) to resource-intensive CNNs that leverage GPUs for enhanced performance.
5. Specialized Applications: A few methods focus on specific use cases, such as organic photovoltaics (OPVs) and material screening using AI-based models to establish structure-property relationships.
6. Datasets and Evaluations: Studies utilize publicly available datasets or create specific datasets to benchmark their models for defect detection accuracy.

These advancements demonstrate the effectiveness of integrating machine learning and deep learning techniques into photovoltaic defect detection but also highlight variations in hardware requirements, dataset availability, and model complexity.

In this paper, we proposed scalable and efficient deep learning model for solar cell defect detection.

3. Methodology

In this part, the design of proposed D-CNN-WT-P-LSTM model presented. Fig.1 depicts the architecture of proposed system.

As showing in figure.1, the proposed model steps are:

1 - Training Phase:

- **Raw Solar Images**: Raw images of solar cells are collected as input for training the system.
- **Distortion Correction**: Training includes applying a distortion correction algorithm to reduce noise and geometric distortions in the images, ensuring accurate feature extraction.
- **Contrast Enhancement**: Images undergo contrast enhancement to improve visibility of defects and enhance the quality of extracted features.
- **Automatic Features Learning (CNN-Layers Features)**: A CNN automatically learns features from the processed images, producing a set of feature maps (F1, F2, ..., Fn).

2 - Testing Phase:

- **Raw Test Image**: A new test image is input into the system for defect detection.
- **Distortion Correction**: The same distortion correction process is applied to the test image for consistency with the training phase.
- **CNN Features Extraction**: Features are extracted from the corrected image using the trained CNN.
- **Wavelet Transform**: The CNN features are transformed using the WT to extract additional spatial and frequency information (W1, W2, ..., Wn).
- **PCA Reduction**: PCA is applied to reduce the dimensionality of the transformed features into a smaller feature set (P1, P2, ..., Pn), making it computationally efficient.
- **LSTM Classification**: The reduced features are input into LSTM network for sequence-based classification, identifying defect types.

3 - Output:

- **Softmax Layer**: The LSTM output passes through a Softmax layer to assign probabilities to defect categories.
- **Defect Detection and Classification Results**: The system outputs the type and likelihood of detected defects.
- **Post-Processing**: Final results are refined, and any additional adjustments are made for enhanced accuracy and usability

3.1 Pre-processing

The image acquired by the EL-imagine devices may suffer from the challenges such as distortions, poor contrast, noise and artefacts while collecting the solar panel images. Existing techniques directly works on such images for defect prediction which leads to incorrect or misclassification problems. To overcome such challenges, in this paper we presented the pre-processing algorithm that overcomes the problems of EL images. Algorithm 1 shows the pre-processing of input solar cell images.

As showing in Algorithm 1, we first applied the Laplacian operator for focus estimation of input image. The Laplacian operation on input cell image results into focused areas with important intensity change. In order to reduce the noise sensitivity, this Laplacian approach is commonly employed in image smoothing processes. This feature accepts a 2-D grayscale image with I as input and provides output as the filtered greyscale (2-D). A picture with pixel intensity values $I\ (p,q)$ has the following Laplacian $LF\ (p,q)$:

$$LF\ (p,q) = \nabla^2\ \frac{\partial^2 I}{\partial p^2} + \frac{\partial^2 I}{\partial q^2} \tag{1}$$

Where, ∇^2 represents the convolutional filter and ∂ sigma value used to construct filter in range between 0 to 1 only. The p and q stand for the position of image pixels. The focused image I^F returned by the LF function. The outcome of LF function passed to the flat field correction.

Algorithm 1: Solar Cell Image Pre-processing

Input
I: $input\ solar\ cell\ raw\ image$
T: $threshold\ value\ of\ appling\ median\ filtering$
σ: $sigma\ value\ for\ Gaussian\ filtering$
Output
I^P: $pre-processed\ solar\ cell\ image$
Select input raw image I
I^F: Apply the Laplacian operation using Eq. (1)
Flat Field correction function on I^F:
$I^{FC} = Gaussian\ (I^F, \sigma)$
Artefact removal using median filtering:
$I^M = median\ (I^{FC})$
I^M: Apply thresholding using Eq. (2)
Adaptive pixel intensity and contrast adjustment
$I^P = imadjust(I^M)$
Return (I^P)

The flat field correction performed using the Gaussian smoothing with a standard deviation of sigma to approximate the shading component of I^F.

After correcting the flat field, the corrected image I^{FC} may have the artefacts, thus we applied the median filtering to remove such artefacts.

A pure median filter responds to features in the image; therefore, we designed the threshold median filter to remove the outliers. A median filtered image I^M is produced for this purpose. All pixels are set to the median filtered value if their relative divergence from the provided image is greater than a threshold:

$$I^{FC}\left[T < \frac{I^{FC} - I^M}{I^M}\right] = I^M \tag{2}$$

After removing the artefact, we applied the function of adaptive contrast enhancement function in which the poor contrast pixels automatically adjusted. This can be done by using the $imadjust$ function of matlab. The final pre-processed image returns as I^P.

3.2 CNN-WT-P-LSTM model

After pre-processing the input solar cell images, the proposed methodology applies a CNN-LSTM-based model for feature extraction and classification. CNN is used for automatic feature learning, while LSTM handles the classification. To enhance performance, the method incorporates WT to refine the high-dimensional features extracted by CNN, making them more robust. Additionally, PCA is employed for feature reduction, reducing computational complexity and improving classification accuracy. The combined model, referred to as CNN-WT-P-LSTM, integrates robust feature extraction (CNN-WT-P) with efficient classification (LSTM).

3.2.1. CNN-WT-P

On each pre-processed cell image I^P , the automated featured extraction of CNN applied in which the image processed through 5 CNN layers to estimate the 2-D features vector of size 128 x 128 of each image followed by the max pooling operation applied on those features. The output of a max-pooling layer is transmitted together with an additive bias through one squashing function that integrates the convolution layer and the pooling layer:

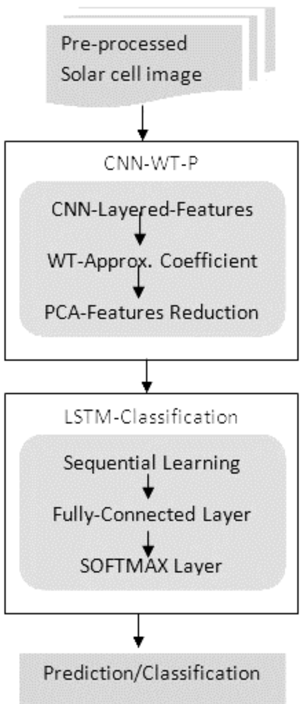

Figure. 2 Architecture of deep learning framework using CNN and LSTM

$$Y_j^l = tanh\left(pooling_{max}\left(\sum_i y_j^{l-1} * kij\right) + b_j^l\right) \quad (3)$$

Where:

Y_j^l: the convolutional layer generates the feature maps l,

y_j^{l-1} : the convolutional layer generates the feature maps, $l-1$,

kij: are the i trained convolution kernels

b_j^l: the additive bias

$pooling_{max}(\cdot)$: the max-pooling operation

$tanh(\cdot)$: The hyperbolic activation function.

The Y_j^l is 2-D feature map produced by the CNN layers which is assigned to F vector. On F we applied the 2-DWT operation to extract the approximation coefficient. The DWT applied on F using 'Haar' wavelet transform as:

$$[Ax, Dx] = 2DWT\ (F, \text{'}haar\text{'}) \quad (4)$$

$$W = Ax \quad (5)$$

Where, $Ax\ and\ Dx$ are approximation and detailed wavelet coefficients respectively of size 64x64. The approximation coefficient used to estimate the final feature vector by applying the PCA function:

$$P = mean(pca(W)) \quad (6)$$

3.2.2. LSTM-classification

The input and output gates, forget gate, peephole connections, and memory blocks that are controlled by memory cells make up the hidden LSTM units. The classification of the input features was carried out by the LSTM model using sequential learning, fully connected layers, and SOFTMAX operations. Using the input feature vector, $F == P$. The equations below explain the activations of a memory block of the hidden LSTM layers. $F == P$.

$$i_t = \sigma(F^t\, W_{Fi} + h_{t-1}W_{hi} + c_{t-1}W_{ci} + b_i) \quad (7)$$

$$f_t = \sigma\left(F^t\, W_{Ff} + h_{t-1}W_{hf} + c_{t-1}W_{cf} + b_f\right) \quad (8)$$

$$o_t = \sigma(F^t\, W_{Fo} + h_{t-1}W_{ho} + c_{t-1}W_{co} + b_o) \quad (9)$$

$$c_t = f_t \diamond c_{t-1} + i_t \diamond \tanh(F^t W_{Fc} + h_{t-1}W_{hc} + b_c) \quad (10)$$

$$h_t = o_t \diamond tanh\ (c_t), \quad (11)$$

Where:

F^t is the input to the LSTM block,

$i_t, f_t, o_t, c_t, and\ h_t$ Are the input gate, the forget gate, the output gate, the cell state and the output of the LSTM block, respectively, at the current time step t.

W_{Fi} , W_{Ff} W_{Fo} are the corresponding weights between the input layer and the input gate, forget gate, and output gate.

W_{hi} , W_{hf} W_{ho} are respectively, the weights between the input gate, forget gate, and output gate of the memory block's hidden recurrent layer.

W_{ci} , W_{cf} , W_{co} are respectively, the weights between the cell state and the input gate, forget gate, and output gate.

b_i ,b_f b_o are respectively, the input gate, forget gate, and output gate additive biases.

The sigmoid function $\sigma(\cdot)$ element-wise multiplication, and hyperbolic activation function $tanh\ (\cdot)$ make up the set of activation functions.

The output features were classified to one of the dataset classes by the fully connected layer and SoftMax layer.

3.3 Post-processing

Once the detection process identifies a solar cell image as defective, post-processing operations are applied. These operations utilize masking and image difference functions to highlight the defective areas within the image. Post-processing is only performed on defective cell images to visually emphasize the specific regions of interest, improving defect localization and interpretation.

4. Experimental analysis

The experimental results of proposed model conducted using the MATLAB tool. The simulation results and their evaluations using different existing methods presented in this section. The results of proposed D-CNN-WT-P-LSTM model compared with existing methods such as:

Conventional Classifiers: ANN and SVM

Basic Deep Learning Classifier: CNN

State-of-art recent methods: Sergiu et.al [24] and Deep Convolutional Neural Network (DCNN) [25]

Then compare with different new models as illustrated in the result tables.

A. Dataset: To evaluate the performance of proposed method and existing methods, we used the publicly available solar cell images [26,27]. The solar cells were extracted from the EL images two types

Received: October 23, 2024. Revised: December 15, 2024.

Table 1. Two class solar cell training dataset

Parameter	No. of images
Normal Samples	1508
Defected Samples (0.33, 0.66, 1.0)	1116
Total Samples	2624

Table 2. Four class solar cell training dataset

Parameter	Number of images
0 Probability	1508
0.33 Probability	295
0.66 Probability	106
1.0 Probability	715
Total Samples	2624

such as polycrystalline and monocrystalline PV modules [26]. Total 2624 solar images are available in dataset with each image of size 300x300.In this research we build the training dataset in two different labels as showing table 1 and 2. According to this, the performances measured for both types of datasets in this paper. In this dataset, each image is labelled with probability of defect such as 0, 0.33, 0.66, and 1.0. All non-zero-defect probability labels are defected images. The defect types are: Cracks, Broken Fingers, Dislocations, Shunts, Black Spots or Stains, PID (Potential-Induced Degradation), Busbar Corrosion, and Inactive or Dead Regions

B. Performance Metrics: Dataset is divided into the ratio of 80 % training and 20 % in this study, to evaluate the performance of proposed model and existing models. The performances are measured in terms of precision rate, recall rate, specificity rate, and accurate rate. The parameters such as True Positive (TP), True Negative (TN), False Positive (FP), and False Negative (FN) are used to compute these results.

$$Precision = \frac{TP}{TP+FP} \tag{12}$$

$$Recall = \frac{TP}{TP+FN} \tag{13}$$

$$Specificity = \frac{TN}{TN+FP} \tag{14}$$

$$Accuracy = \frac{TP+TN}{TP+TN+FP+FN} \tag{15}$$

C. Comparative Results: This section presents the comparative results by considering both 2-Class and 4-Class datasets using the different methods discussed above.

Table 3 shows the outcome of accuracy, precision, and recall rates respectively. Among all those methods the proposed model D-CNN-WT-P-LSTM achieved the significant performance improvement over the conventional classifiers ANN and SVM, basic deep learning classifier CNN, and recent deep learning based solar cell defect methods such as Sergiu et.al and DCNN considering both 2-Class and 4-Class datasets.

The conventional classifiers ANN and SVM showing the worst accuracy performance among all the methods as it mainly based on the hand-crafted features. The automated features extraction-based technique CNN further shows the better solar cell detection results compared to ANN and SVM considering the precision rate and accuracy rate parameters. The deep learning-based model designed in [24] and [25] shows the improvement in solar cell defect performances compared to ANN, Modified SVM, and CNN models.

Table 3. Results Analysis of different classes

Type	Result	ANN	Modified SVM	CNN	DCNN	L-CNN	Light CNN	DFB-SVM	Hessian Matrix	ResNet152-Xception	VGG-19	Proposed
2-Classes	Accuracy	73.33	81.52	82.10	86.10	90.10	92.00	94.67	94.10	96.00	90.10	98.48
	Precision	76.36	74.55	80.77	82.67	91.45	91.85	96.72	94.13	96.90	93.39	99.20
	Recall	73.68	88.89	79.41	81.46	93.59	96.18	95.68	97.12	95.06	91.20	98.67
	Specificity	72.92	75.60	84.32	89.06	83.52	84.32	92.26	88.20	96.95	88.04	98.00
4-Classes	Accuracy	76.00	83.62	85.14	83.05	88.38	93.90	94.29	92.19	96.38	93.90	94.10
	Precision	78.62	78.14	85.90	79.52	89.68	93.82	95.70	94.63	97.74	92.93	95.83
	Recall	76.41	89.71	81.71	78.40	92.12	96.67	95.70	93.24	96.19	96.17	94.99
	Specificity	75.52	78.37	88.17	86.22	82.05	89.23	91.48	90.27	96.67	91.18	92.47

Received: October 23, 2024. Revised: December 15, 2024.

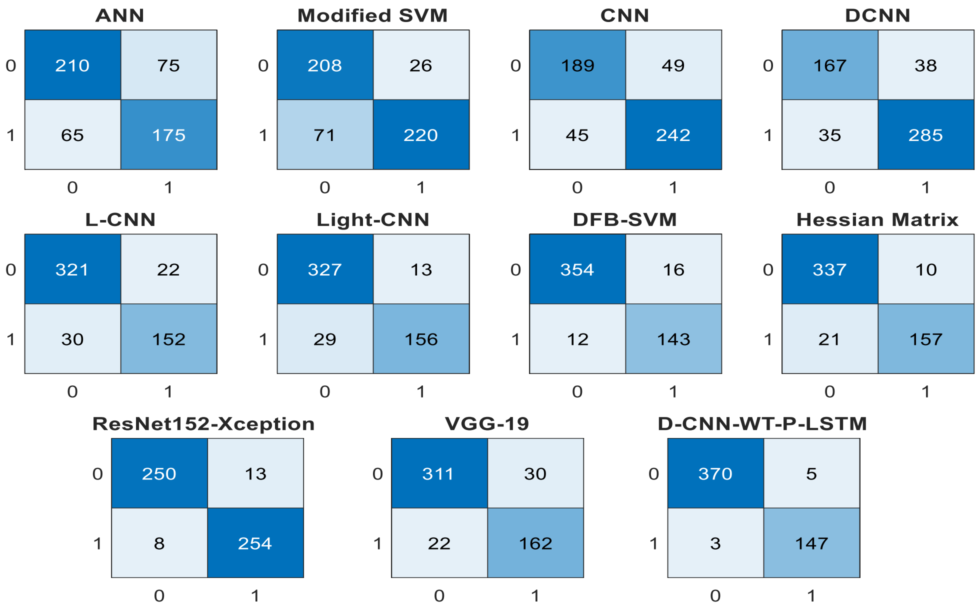

Figure. 3 Confusion matrix comparison for 2-Classes

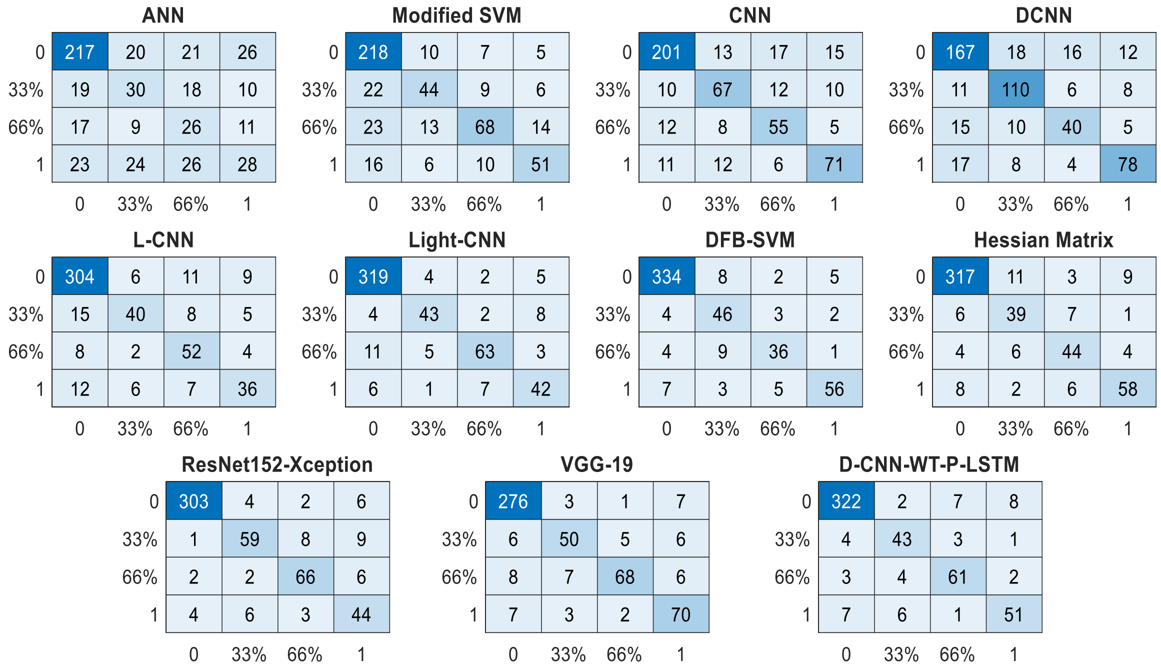

Figure. 4 Confusion matrix comparison for 4-Classes

The specificity rate further justified the correctness ratio improvement of proposed method over the existing methods. The D-CNN-WT-P-LSTM results demonstrate efficiency of solar cell detect detection and classification compared to all existing methods due to points (1) inclusion of effective pre-processing

step where the distorted and poor-quality solar cell images enhanced which is missing with existing deep learning-based methods like CNN, recent works Sergiu et.al. and DCNN, (2) optimized features extraction and reduction process at CNN module using the wavelet transform and PCA provides the more robust features compared existing solutions, and (3) last but not the least, the use of LSTM module for the classification purpose overcomes the problems of computational efficiency compared to individual CNN module for the automatic features extraction and classification.

Table 4. Comparison Average Accuracy Results with Relevant Works from Literature.

Ref.	Method	Accuracy
[3]	ANN	74.67%
[24]	Modified SVM	82.57%
[22]	CNN	83.62%
[25]	DCNN	84.57%
[27]	L-CNN	89.24%
[21]	Light CNN	92.95%
[27]	DFB-SVM	94.48%
[28]	Hessian Matrix	93.14%
[29]	ResNet152-Xception	96.19%
[22]	VGG-19	92%
Proposed	D-CNN-WT-P-LSTM	96.29%

The confusion matrix of 2-class and 4-class were illustrated in Fig. 3, and Fig.4. The evaluated models are ANN, Modified, CNN, DCNN, L-CNN, Light-CNN, DFB-SVM, Hessian Matrix, ResNet152-Xception, VGG-19, and the proposed model (D-CNN-WT-P-LSTM)

The comparative Table 4 shows the accuracy achieved by different methods for photovoltaic cell defect detection. The average is computed by combining the 2-Class and 4-Class dataset accuracy results. As showing the highest accuracy achieved by the proposed model D-CNN-WP-LSTM. In this table we included another variant without using the WT-P called D-CNN-LSTM to demonstrate the effect of improving the CNN features extraction process.

As shown in Table 4 the proposed D-CNN-WT-P-LSTM method achieves the highest accuracy of 96.29%, slightly surpassing ResNet152-Xception. This improvement is due to the integration of:

- Wavelet Transform (WT): Effective for signal and frequency analysis.
- Parallel LSTM: Enhances temporal feature extraction and sequence modelling, providing an edge for tasks requiring temporal dependency analysis.

5. Conclusion and future work

The D-CNN-WT-P-LSTM framework is proposed for defect detection in solar cell EL images, incorporating pre-processing, feature extraction, classification, and post-processing steps. It effectively addresses challenges like distortions and noise while leveraging the combined strengths of CNN and LSTM for improved classification accuracy. The framework outperforms existing methods, achieving 14%-20% and 11%-13% higher accuracy for 2-class and 4-class classifications compared to CNN and DCNN models, with an additional 2% improvement over ResNet152-Xception. These results highlight the framework's robustness and potential. Future work will explore other deep learning techniques to further enhance defect detection.

Notations

Variables	Description
∇^2	Convolutional filter
∂	Sigma value used to construct filter
p and q	Stand for the position of image pixels.
I^F	focused image
LF	Flat field correction function
I^M	Median filtered image
T	Threshold of Appling median filtering
σ	Sigma value for Gaussian Filtering
I^P	Pre-Processed solar cell image
Y_j^l	Convolutional layer generates the maps l
y_j^{l-1}	Convolutional layer generates the maps $l-1$
kij	The i trained convolution kernels
$pooling_{max}$	Max-pooling operation
$tanh(\cdot)$:	Hyperbolic activation function.
$Ax\ and\ Dx$	Approximation and detailed wavelet coefficients respectively
F^t	Input to the LSTM block
$i_t, f_t, o_t, c_t, and\ h_t$	The input gate, the forget gate, the output gate, the cell state and the output of the LSTM block, respectively
W_{Fi},W_{Ff} W_{Fo}	Respectively, the weights between the input gate, forget gate, and output gate of the memory block's hidden layer
b_i,b_f b_o	Respectively, the input gate, forget gate, and output gate additive biases.
TP	True Positive
TN	True Negative
FP	False Positive
FN	False Negative

Conflicts of Interest

The authors declare no conflict of interest.

Author Contributions

Conceptualization, methodology, formal analysis, writing original draft, R.A; supervision, resources, project administration, G.C.H.; project administration, validation, F.H.N.; proofreading, reviewing and editing the draft copy, H.N.A; reviewing and editing the draft copy, Z.A. A.

References

[1] F. Spertino *et al.*, "A power and energy procedure in operating photovoltaic systems to quantify the losses according to the causes", *Solar Energy*, Vol. 118, pp. 313-326, 2015.

[2] I. Berardone, J. Lopez Garcia, and M. Paggi, "Quantitative analysis of electroluminescence and infrared thermal images for aged monocrystalline silicon photovoltaic modules", In: *Proc. of 2017 IEEE 44th Photovoltaic Specialist Conference (PVSC)*, pp. 402-407, 2017.

[3] T. H. Luu, P. N. Ky Phuc, T. Lam, Z. Yu, and V. T. Lam, "Ensembling techniques in solar panel quality classification", *International Journal of Electrical and Computer Engineering (IJECE)*, Vol. 13, No. 5, p. 5674, Oct. 2023.

[4] I. Berardone, M. Corrado, and M. Paggi, "A Generalized Electric Model for Mono and Polycrystalline Silicon in the Presence of Cracks and Random Defects", *Energy Procedia*, Vol. 55, pp. 22-29, 2014.

[5] M. Paggi, M. Corrado, and I. Berardone, "A global/local approach for the prediction of the electric response of cracked solar cells in photovoltaic modules under the action of mechanical loads", *Engineering Fracture Mechanics*, Vol. 168, pp. 40-57, 2016.

[6] M. Alsafasfeh, I. Abdel-Qader, and B. Bazuin, "Fault detection in photovoltaic system using SLIC and thermal images", In: *Proc. of 2017 8th International Conference on Information Technology (ICIT)*, pp. 672-676, 2017.

[7] M.-P. Song, X.-D. Shang, C.-Y. Yu, J.-B. An, and C.-I. Chang, "Research On Broken Corner And Black Edge Detection Of Solar Cell", In: *Proc. of 2018 International Conference on Machine Learning and Cybernetics (ICMLC)*, pp. 80-84, 2018.

[8] Y. Li, H. Huang, Q. Xie, L. Yao, and Q. Chen, "Research on a Surface Defect Detection Algorithm Based on MobileNet-SSD", *Applied Sciences*, Vol. 8, No. 9, p. 1678, 2018.

[9] M. Alt, S. Fischer, S. Schenk, S. Zimmermann, K. Ramspeck, and M. Meixner, "Electroluminescence imaging and automatic cell classification in mass production of silicon solar cells", In: *Proc. of 2018 IEEE 7th World Conference on Photovoltaic Energy Conversion (WCPEC) (A Joint Conference of 45th IEEE PVSC, 28th PVSEC & 34th EU PVSEC)*, pp. 3298-3304, 2018.

[10] H. Chen, J. Liu, S. Wang, and K. Liu, "Robust Dislocation Defects Region Segmentation for Polysilicon Wafer Image With Random Texture Background", *IEEE Access*, Vol. 7, pp. 134318-134329, 2019.

[11] K.-M. Lin, H.-H. Lin, H. K. Dandage, and Y.-C. Du, "Pseudo colorization of electroluminescence images of multi-crystalline silicon solar cells for defect inspection", *Modern Physics Letters B*, Vol. 33, No. 14n15, p. 1940010, 2019.

[12] B. Su, H. Chen, Y. Zhu, W. Liu, and K. Liu, "Classification of Manufacturing Defects in Multicrystalline Solar Cells With Novel Feature Descriptor", *IEEE Transactions on Instrumentation and Measurement*, Vol. 68, No. 12, pp. 4675-4688, 2019.

[13] F. Li *et al.*, "Machine Learning (ML)-Assisted Design and Fabrication for Solar Cells", *ENERGY & ENVIRONMENTAL MATERIALS*, Vol. 2, No. 4, pp. 280-291, 2019.

[14] M. Mayr, M. Hoffmann, A. Maier, and V. Christlein, "Weakly Supervised Segmentation of Cracks on Solar Cells Using Normalized L p Norm", In: *Proc. of 2019 IEEE International Conference on Image Processing (ICIP)*, 2019.

[15] C. Mantel *et al.*, "Machine learning prediction of defect types for electroluminescence images of photovoltaic panels", *Applications of Machine Learning*, Vol.11139, p. 1-9, 2019.

[16] Y. S. Balc?o?lu, B. Sezen, and C. Cubukcu Cerasi, "Solar Cell Busbars Surface Defect Detection Based on Deep Convolutional Neural Network", *IEEE Latin America Transactions*, Vol. 21, No. 2, pp. 242-250, 2023.

[17] B. Ni, P. Zou, Q. Li, and Y. Chen, "Intelligent Defect Detection Method of Photovoltaic Modules Based on Deep Learning", *Advances in Intelligent Systems Research*, Vol. 161, p. 167-173, 2018.

[18] A. Bartler, L. Mauch, B. Yang, M. Reuter, and L. Stoicescu, "Automated Detection of Solar Cell Defects with Deep Learning", In: *Proc. of 2018 26th European Signal Processing Conference (EUSIPCO)*, pp. 2035-2039, 2018.

[19] H. Chen, Y. Pang, Q. Hu, and K. Liu, "Solar cell surface defect inspection based on multispectral convolutional neural network", *Journal of Intelligent Manufacturing*, Vol. 31, No. 2, pp. 453-468, 2020.

[20] M. Sun, S. Lv, X. Zhao, R. Li, W. Zhang, and X. Zhang, "Defect Detection of Photovoltaic Modules Based on Convolutional Neural

Received: October 23, 2024. Revised: December 15, 2024.

Network", *Lecture Notes of the Institute for Computer Sciences, Social Informatics and Telecommunications Engineering*, Vol. 226, pp. 122-132., 2018,

[21] M. W. Akram *et al.*, "CNN based automatic detection of photovoltaic cell defects in electroluminescence images", *Energy*, Vol. 189, p. 116319, 2019.

[22] R. A. I. Almashhadani, G. C. Hock, F. H. Bt Nordin, and H. N. Abdulrazzak, "Electroluminescence Images for Solar Cell Fault Detection Using Deep Learning for Binary and Multiclass Classification", *International Journal of Electrical and Electronics Engineering*, Vol. 11, No. 5, pp. 150-160, 2024.

[23] W. Sun *et al.*, "Machine learning-assisted molecular design and efficiency prediction for high-performance organic photovoltaic materials", *Science Advances*, Vol. 5, No. 11, 2019.

[24] S. Deitsch *et al.*, "Automatic classification of defective photovoltaic module cells in electroluminescence images", *Solar Energy*, Vol. 185, pp. 455-468, 2019.

[25] R. Pierdicca, E. S. Malinverni, F. Piccinini, M. Paolanti, A. Felicetti, and P. Zingaretti, "Deep Convolutional Neural Network for Automatic Detection of Damaged Photovoltaic Cells", *The International Archives of the Photogrammetry, Remote Sensing and Spatial Information Sciences*, Vol. XLII-2, pp. 893-900, 2018.

[26] S. Deitsch *et al.*, "Segmentation of photovoltaic module cells in uncalibrated electroluminescence images", *Machine Vision and Applications*, Vol. 32, No. 4, p. 84, 2021.

[27] M. Y. Demirci, N. Beşli, and A. Gümüşçü, "Efficient deep feature extraction and classification for identifying defective photovoltaic module cells in Electroluminescence images", *Expert Systems with Applications*, Vol. 175, p. 114810, 2021.

[28] W. Tang, Q. Yang, X. Hu, and W. Yan, "Convolution neural network based polycrystalline silicon photovoltaic cell linear defect diagnosis using electroluminescence images", *Expert Systems with Applications*, Vol. 202, p. 117087, 2022.

[29] J. Wang *et al.*, "Deep-Learning-Based Automatic Detection of Photovoltaic Cell Defects in Electroluminescence Images", *Sensors*, Vol. 23, No. 1, p. 297, 2022.